

Xác định phân bố điện áp trên dây quấn của máy biến áp bằng phương pháp biến trạng thái

Đoàn Thanh Bảo¹, Phạm Quốc Vũ², Phạm Trung Duy³

¹Khoa Kỹ thuật và Công nghệ, Trường Đại học Quy Nhơn, Việt Nam

²Điện lực Phù Mỹ, Công ty Điện lực Bình Định, Việt Nam

³Hạt Quản lý giao thông - công chính huyện Phù Mỹ, Bình Định, Việt Nam

Ngày nhận bài: 23/11/2020; Ngày nhận đăng: 30/12/2020

TÓM TẮT

Sự cố quá điện áp thoảng qua ở đầu cực máy biến áp tạo ra dao động điện áp tần số cao xâm nhập vào máy biến áp. Những dao động này có thể gây ra thiệt hại cho cách điện của máy biến áp. Đây thuộc dạng sự cố nặng nề, khó khắc phục và sửa chữa. Chính vì vậy, việc bảo vệ quá áp cho máy biến áp trở thành một vấn đề cấp thiết. Bài báo đã chỉ ra rằng việc sử dụng dây quấn đan xen có điện dung nối tiếp giữa các bánh dây lớn hơn dây quấn xoắn ốc liên tục, có tác dụng phân bố đều điện áp giữa các bánh dây và làm tăng khả năng chịu quá áp. Đồng thời, bài báo đã xác định điện áp trên từng vị trí của bối dây khi chịu xung sét tác động vào đầu cực máy biến áp và phân bố điện áp trên cuộn dây đan xen tại thời điểm khi xung sét có giá trị cực đại. Từ đó kết luận về tính hiệu quả của phương pháp quấn dây đan xen khi sử dụng làm dây quấn máy biến áp.

Từ khóa: Quá điện áp, dây quấn đan xen, máy biến áp, xung sét, điện dung.

*Tác giả liên hệ chính.

Email: dtbao@ftt.edu.vn

Determination of voltage distribution on winding of transformer by state variable method

Doan Thanh Bao^{1,*}, Pham Quoc Vu², Pham Trung Duy³

¹*Faculty of Engineering and Technology, Quy Nhon University, Vietnam*

²*Phu My power, Binh Dinh power company, Vietnam*

³*Traffic management station - Public works, Phu My district, Binh Dinh, Vietnam*

Received: 23/11/2020; Accepted: 30/12/2020

ABSTRACT

A transient overvoltage incident at the transformer terminal generates high-frequency voltage fluctuations that have negative impacts on the transformer. These oscillations may cause damage to the insulation of transformers. It is difficult to restore, and repair these serious problems. Therefore, overvoltage protection for the transformers is essential. This paper pointed out that the interleaved disk winding has a larger capacitance than that of continuous disk windings. Therefore, the use of interleaved disk winding has the effect of making the voltage distribution on the winding wheels more even and increasing the overvoltage resistance of the transformer. In addition, the value of the voltage at each position of the winding when lightning impulses on the transformer terminal and the voltage distribution on the interleaved disk winding at the time when the lightning impulse has maximum value are also presented in the article. On that basis, the effectiveness of using the interleaved disk winding method in the transformer will be analyzed in detail.

Keywords: *Over voltage, interleaved disk-type winding, transformer, lightning strike, capacitance.*

1. INTRODUCTION

Among the types of transformer faults, the fault caused by overvoltage is the most serious, difficult to fix and repair. Atmospheric overvoltage usually occurs in a very short period of time, but the voltage applied to the terminal has a great amplitude and slope values which are very dangerous for the transformer windings. Therefore, the overvoltage protection for transformers becomes an urgent issue in the process of designing, manufacturing, testing and operating transformers.¹ The methods of overvoltage protection used today are discharge electrodes, lightning arresters or capacitive rings.²

At industrial electrical frequencies, the role of capacitive elements is negligible and often ignored. When a voltage pulse acts on the terminal of the transformer windings, which contains high-order harmonic elements, the role of the capacitive elements becomes much more significant.³ At this time, the voltage acts on the winding terminals are greatly reduced on a few first gallet. Therefore, these gallets usually increase the insulation or they are connected in parallel with an equipotential electrode known as a capacitive ring.^{4,5}

The capacitive ring works to increase the capacitance of the winding at the terminal position. However, with large capacity

^{*}*Corresponding author.*

Email: dtbao@fit.edu.vn

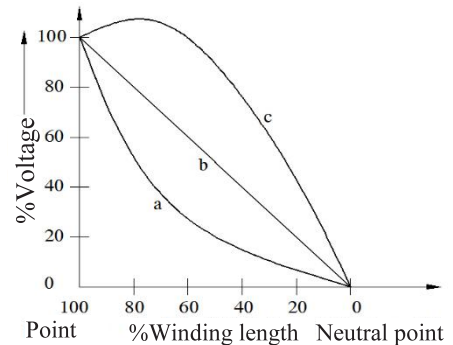
transformers, high voltage and high production costs, it is also necessary to increase the capacitance value of the inner coils. That is the method of interleaved disk winding.^{5,6}

The paper calculated the series and parallel capacitance of types of continuous disk windings and interleaved disk windings when they are of the same geometric size. The results showed that the interleaved disk winding has a greater capacitance than continuous disk winding. Furthermore, the paper used the equivalent circuit model and the state variable method solved on Matlab Simulink software to determine the voltage distribution across the nodes of the winding at the time when the value of lightning impulse voltage is maximum. The distribution of the voltage on the interleaved disk winding at the moment when the lightning impulse is maximum value is also determined by this measure.

2. BUILDING MODEL OF THE WINDING

2.1. Initial voltage distribution

When a voltage pulse acts on the terminals of the transformer winding, the voltage at the initial time distributed in the windings depends on the capacitance between the rings, the capacitance between the winding wheels, the capacitance between the windings each other and between the windings and ground.⁷ The inductance and inductor of the winding have no effect on the initial voltage distribution. Therefore, inductance does not allow current to flow and the voltage distribution is determined by the capacitive network. When the impulse voltage remains for a sufficiently long time (50 - 100 μ s), current begins to flow through the inductance significantly. Eventually, this forms a stable voltage distribution. Thus there is a difference between the initial voltage distribution and the stable voltage distribution, the values of voltage are shown in Figure 1.^{1,4}



a) Initial voltage distribution; (b) The stable voltage distribution;
(c) Maximum voltage

Figure 1. Voltage distribution in the winding^{1,4}

In Figure 1, it is seen that at the beginning, the voltage drops suddenly at a point about 20% of the length of the winding, then slowly decreases in the rest. Hence the intensity of electrical current between the first gaskets of the windings (2 - 5 first gaskets) is much greater than that between the rest of the gaskets. In addition, there are times when the maximum voltage value at a certain point on the windings are greater than the applied voltage. Therefore, in order to increase the ability of overvoltage of the windings, it is necessary to make the initial voltage distribution closer to the stable voltage distribution.⁶

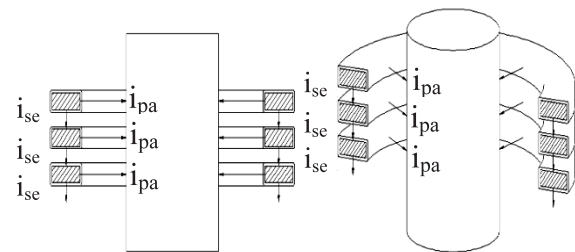


Figure 2. Capacitance current distribution of single-layer winding

The voltage distribution across the rings now depends on the capacitance value of the windings (between windings and ground or between the rings).

Where, C_{se} is the sum of the series capacitance between the rings and the capacitance between the gaskets or the capacitance between

parts of the winding; C_{pa} is the sum of parallel capacitance between the windings and steel core, the capacitance between the windings and the machine shell.

The initial voltage distribution was determined by the distribution coefficient:^{8,9}

$$\alpha = \sqrt{\frac{C_{pa}}{C_{se}}} \quad (1)$$

For different values of α , the initial voltage distribution is shown in Figure 3.

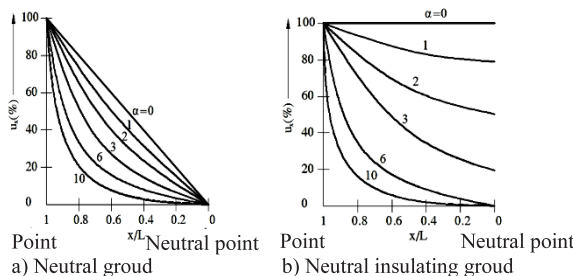


Figure 3. The initial voltage distribution^{1,4}

The coefficient α indicates the deviation of the original voltage distribution line from the stable voltage distribution line. The higher the coefficient α is, the larger the difference is. In order to reduce the distribution coefficient α , there are two ways. One solution is that the value of C_{pa} must be decreased, and another one is that the value of C_{se} must be increased. However, the reduction of value in C_{pa} involves varying the spacing between the strings, which is often fixed by early design requirements. Therefore, it is common to choose to increase C_{se} by changing the winding method. The method of interleaved disk winding is an effective method used today.⁶

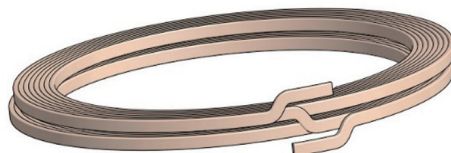


Figure 4. A pair of gallets of interleaved disk winding

Figure 4 shows a simple interleaved disk winding model, consisting of a single 2-gallet

circuit, 8 turns per gallet, the number of turns per gallet equivalent to a spiral winding. However, the performance of winding the interlacing pattern is more complicated because welding is required on each pair of gallet and the insulation between the coils of the winding is also required higher.

2.2. Calculating parallel capacitance

The parallel capacitance between the gallets and the steel core is the capacitance of a cylindrical capacitor with one side being the innermost ring, the other side being the steel core. This capacitor is filled with two dielectric zones, the insulating paper and the transformer oil. Applying the formula to calculate the capacitance of the capacitor in a homogeneous atmosphere the capacitance between two concentric wires, or between the inner coils and the steel core is calculated as follows:^{4,8}

$$C_{pa} = \frac{C_{ins} \cdot C_{oil}}{C_{ins} + C_{oil}} \quad (2)$$

$$\text{with } C_{ins} = \epsilon_0 \cdot \epsilon_{ins} \frac{\pi D_m h}{d_{ins}} \quad (3)$$

$$\text{and } C_{oil} = \epsilon_0 \cdot \epsilon_{oil} \frac{\pi D_m h}{d_{oil}} \quad (4)$$

Where,

D_m is the mean diameter of the gap between the two windings

d_{oil} and d_{ins} are the thickness of the oil and the insulation between the two windings, respectively

h is the height of the wire wheel in the axial direction

ϵ_0 , ϵ_{oil} and ϵ_{ins} are the dielectric constants of the vacuum, the oil and the insulation paper, respectively.

These dimensions are shown in Figure 5

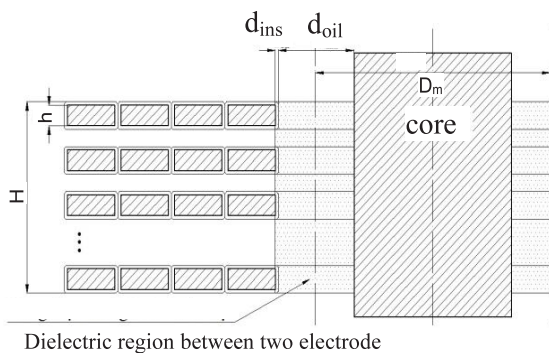


Figure 5. Cross-section of inner winding and core

From (3) and (4), we have:

$$C_{pa} = \frac{\epsilon_0 \pi D_m h}{\frac{d_{ins}}{\epsilon_{ins}} + \frac{d_{oil}}{\epsilon_{oil}}} \quad (5)$$

The formula is used to determine the capacitance between the outer winding and one side of the transformer's shell:

$$C_{pa} = \frac{\epsilon_0 \pi D_m h}{\cosh^{-1}(\frac{s}{R})} \left[\frac{d_{oil} + d_{ins}}{\frac{d_{ins}}{\epsilon_{ins}} + \frac{d_{oil}}{\epsilon_{oil}}} \right] \quad (6)$$

Where,

h and R are the heights and radius of the winding, respectively.

s is the distance from the center of the wire to the shell.

2.3. Serial capacitance calculation

2.3.1. Series capacitance in continuous disk winding

Similar to the calculation of parallel capacitance, the axial capacitance between two physically adjacent galleys is the capacitance of three capacitors connected in series as shown in Figure 6.^{4,10}

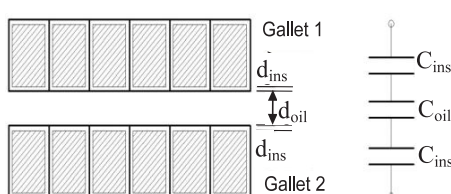


Figure 6. Capacitance between two galleys

The capacitance between coils is calculated by the formula:

$$C_v = \frac{\epsilon_0 \cdot \epsilon_{ins} \pi D_m h}{2d_{ins}} \quad (7)$$

The capacitance of the capacitor, which the dielectric is the insulating paper and the transformer oil, is calculated by the formula:

$$C_{DA} = \frac{\epsilon_0 \pi D_m R}{\frac{2d_{ins}}{\epsilon_{ins}} + \frac{d_{oil}}{\epsilon_{oil}}} \quad (8)$$

Where R is the radial thickness.

Assume that C_v and C_B are capacitance between physically adjacent turns and between two opposite turns of a pair of galleys as shown in Figure 7.

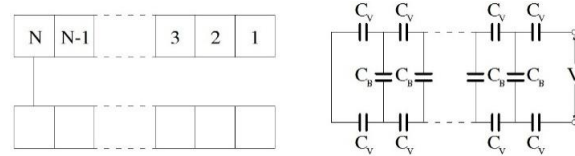


Figure 7. A pair of galleys in continuous disk winding

The total series capacitance of a pair of galleys is:

$$C_{se} = \frac{C_v}{2N^2} (N-1) + \frac{(N-1)(2N-1)C_B}{6N} \quad (9)$$

$$\text{or} \quad C_{se} = \frac{C_v}{2N^2} (N-1) + \frac{C_{DA}}{3} \quad (10)$$

2.3.2. Series capacitance in interleaved disk winding

With the interleaved disk winding shown in Figure 4, the voltage acts on N (turns of a gallet) is $V/2$, and the voltage acts on (N-2) (turns of a gallet) is $[(N-1)/2N]*V$, the total energy in galleys is [2]:

$$E_n = \frac{1}{2} C_v \left(\frac{V}{2} \right)^2 N + \frac{1}{2} C_v \left(\frac{N-1}{2N} V \right)^2 (N-2) \quad (11)$$

$$\text{In addition to this: } E_n = \frac{1}{2} C_{Vtd} V^2$$

Therefore, we have:

$$C_{Vtd} = \frac{C_v}{4} \left[N + \left(\frac{N-1}{N} \right)^2 (N-2) \right]$$

If $N \gg 1$, the series capacitance between the two wire wheels is:

$$C_{se} = C_{Vtd} = \frac{C_v}{2}(N-1) \quad (12)$$

2.4. Calculation of inductance between the rings

The formula for calculating the inductance between two rings have the small cross-section, coaxial is calculated by [3] [4]:

$$L_{AB} = \frac{2\mu_0}{k} N_A \cdot N_B \sqrt{R_A R_B} \left\{ \left[1 - \frac{k^2}{2} \right] K(k) - E(k) \right\} \quad (13)$$

Where,

$$k = \sqrt{\frac{4R_A R_B}{(R_A + R_B)^2 + S^2}}$$

R_A , R_B are the radius of the two winding A and B, respectively

S is the distance between the two rings

N_A and N_B are the number of winding A and wingding B, respectively

$K(k)$ and $E(k)$ are complete elliptic integrals of types 1 and 2.

$$K(k) = \int_0^{\frac{\pi}{2}} \frac{d\theta}{\sqrt{1-k^2 \sin^2 \theta}} \quad \text{and} \quad E(k) = \int_0^{\frac{\pi}{2}} \sqrt{1-k^2 \sin^2 \theta} d\theta$$

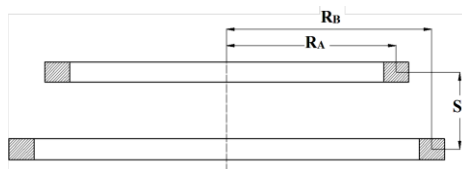


Figure 8. Cross section of two coaxial rings

3. CALCULATION OF VOLTAGE DISTRIBUTION

3.1. Equivalent circuit model

The equivalent circuit model of the transformer windings is depicted in Figure 9. Conductor G has an extremely small value and does not affect the initial voltage distribution, because at the initial moment the current flowing through

the inductor is almost zero, only current flows through capacitance.

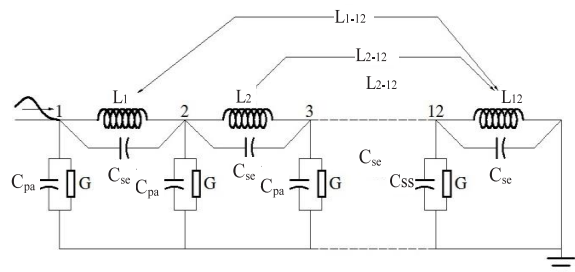


Figure 9. Equivalent circuit of the windings

The equivalent circuits include the following components:

C_{se} is the series capacitance between the wire wheels,

C_{pa} is the parallel capacitance between the wire wheels,

L_i , L_{ij} are the inductance of the wire wheels and the mutual inductance between the wire wheels, respectively,

G is conductance of the wire wheels.

Considering of an transformer with following parameters, $S = 2.200 \text{ kVA} - 22/0.4 \text{ kV}$. Wire wheel dimensions (in centimetres) of this transformer are shown in Figure 10.

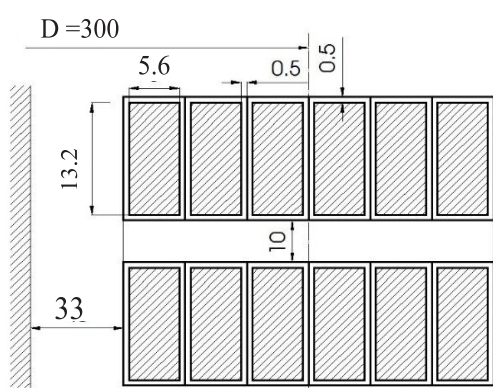


Figure 10. Surveyed transformer's dimensions of wire wheel

Using equations (2), (10) and (12) to calculate for transformer whose parameters are supplied in Figure 10, obtained results are shown in Table 1.

Table 1. Parallel and series capacitance

Obtained results	C_{pa} (Parallel capacitance)	C_{secw} (Series capacitance in a continuous disk winding type)	C_{seiw} (Series capacitance in interleaved disk winding)
Capacitance (F)	$0.551*10^{-7}$	$1.46*10^{-7}$	$36.0*10^{-7}$

Similarly, using equation 13 to calculate for transformer whose parameters are supplied in Figure 10, results calculated by Matlab/Simulinks software are shown in Table 2.

Table 2. The inductance of the wire wheels and the mutual inductance between them (the unit of measure is the Herry)

$L_{1-1} = 5.1957*10^{-5}$	$L_{1-5} = 2.1926*10^{-5}$	$L_{1-9} = 1.5060*10^{-5}$
$L_{1-2} = 3.6287*10^{-5}$	$L_{1-6} = 1.9575*10^{-5}$	$L_{1-10} = 1.4076*10^{-5}$
$L_{1-3} = 2.9391*10^{-5}$	$L_{1-7} = 1.7733*10^{-5}$	$L_{1-11} = 1.3262*10^{-5}$
$L_{1-4} = 2.5033*10^{-5}$	$L_{1-8} = 1.6258*10^{-5}$	$L_{1-12} = 1.2584*10^{-5}$

3.2. Calculation of voltage distribution by the state variable method

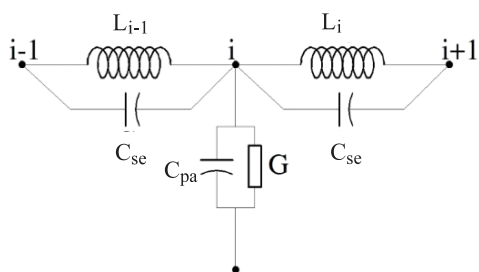


Figure 11. Any node from an equivalent circuit

Choose a random node from the equivalent circuit shown in Figure 11.

The general equation of the equivalent circuit is shown as follows [4]:

$$\hat{C}\ddot{y}(t) + \hat{G}\dot{y}(t) + \hat{F}\hat{y}(t) = 0 \quad (14)$$

Where,

\hat{C} is the node capacitance matrix,

\hat{G} is the node conductance matrix,

\hat{F} is the inverse node inductance matrix, $\hat{y}(t)$ is the voltage vector at the nodes.

The relationship between the node matrices and the branch matrices is shown as follows:

$$\hat{C} = Q_C C_b Q_C^T \quad (14a)$$

$$\hat{G} = Q_G G_b Q_G^T \quad (14b)$$

$$\hat{F} = Q_L L_b^{-1} Q_L^T \quad (14c)$$

Where, Q_C , Q_L and Q_G are interdependent matrices between the node and branch with capacitance, inductance and conductivity. C_b , L_b , G_b are the branch capacitance matrix, inductance matrix and branch inductance matrix, respectively.

3.2.1. State variable model

The system of equations of state variables describing the voltage distribution in the transformer is shown in Equation 15

$$\begin{aligned} \dot{X}(t) &= AX(t) + Bv(t) \\ y(t) &= FX(t) + Dv(t) \end{aligned} \quad (15)$$

Where,

$X(t)$ is state variable vector,

A , F are constant coefficient matrix,

F , D are column matrix of the constant coefficients,

$v(t)$ is input pulse voltage vector,

$y(t)$ is output node voltage vector.

3.2.2. Input voltage block

The voltage applied to the winding terminals is assumed to be a standard lightning impulse voltage 1/50. This is the most common type of lightning wave and causes many problems for lines and transformer stations. The values of lightning impulse voltages are expressed algebraically as follows:

$$x(t) = 1,0167U(e^{-0,01423t} - e^{-6,6091t}) \quad (16)$$

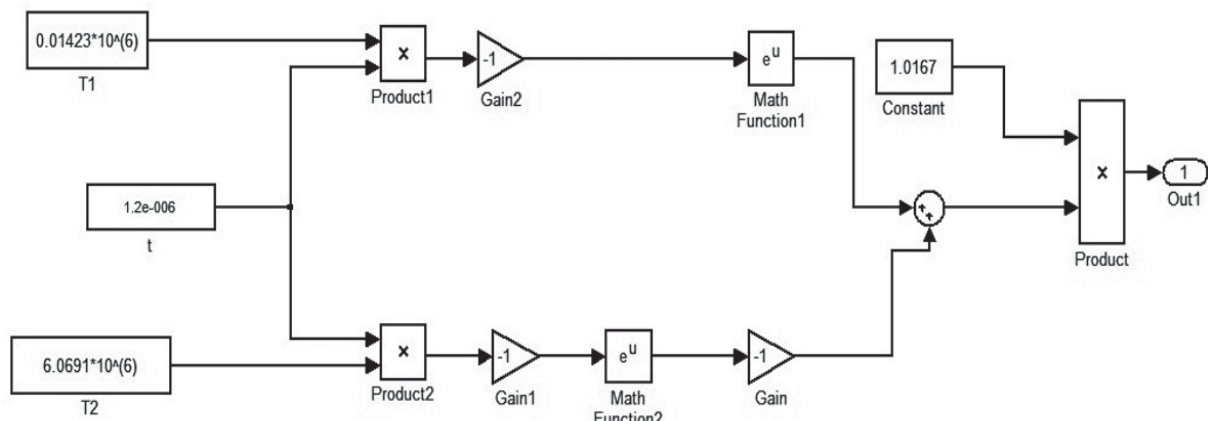


Figure 12. Lightning impulse voltage stimulating block

To build the input voltage model, blocks in the Matlab/Simulink software are used. The output of the block model (Figure 12) is the unit lightning impulse voltage value. This result is shown in Figure 13.

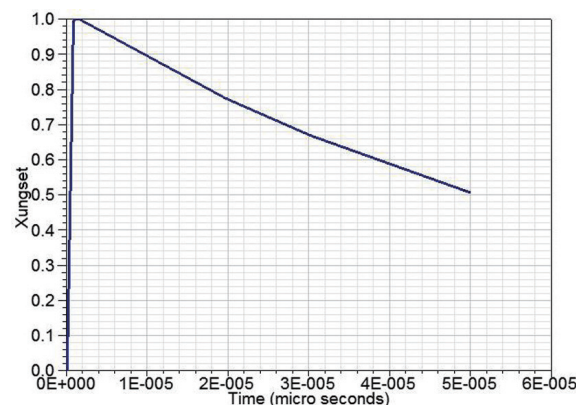


Figure 13. Type of output voltage of lightning impulse block

3.2.3. Simulation model

Parametric matrices A, B, F, D in the system of equations 15 are solved by matlab programming code. State-Space blocks and sub-blocks are also built on Matlab Simulink software. The full simulation diagram is shown in Figure 14.

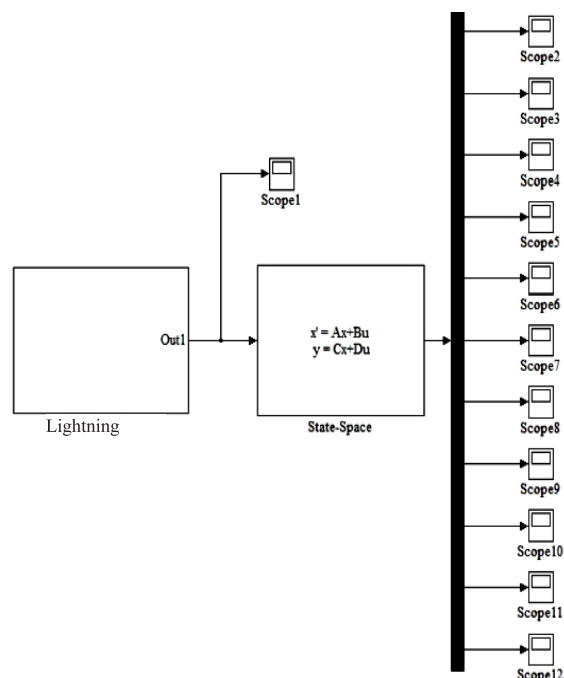


Figure 14. Full block diagram in Matlab Simulink software

The simulation diagram in the Matlab Simulink software (Figure 14) is used to determine the voltage distribution on both continuous disk windings and interleaved disk winding.

3.2.4. Obtained simulation results for continuous disk winding

Table 3. Voltage values at 12 nodes on continuous disk winding

Node 1	Node 2	Node 3	Node 4	Node 5	Node 6
1.0000	0.3023	0.0906	0.0275	0.0076	0.0021
Node 7	Node 8	Node 9	Node 10	Node 11	Node 12
0.0007	0.0002	0.0001	0.0001	0.0001	0.0002

The obtained simulation result of the voltage at node 2 of the continuous disk winding is showed in Figure 15.

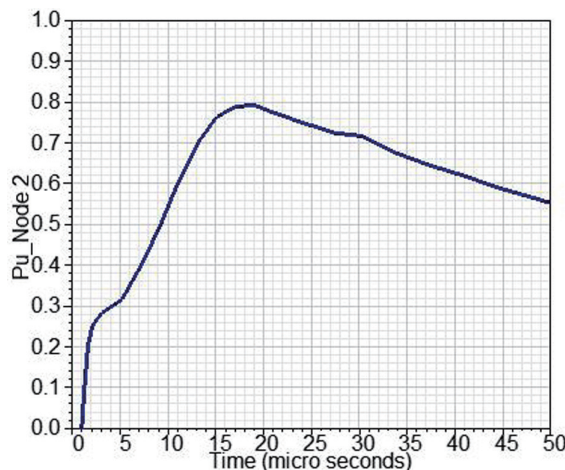


Figure 15. The voltage at node 2 - Type of continuous disk winding

Similarly, Table 3 shows the simulation results of voltage values at the remaining 11 nodes at the time of 50 μ s. The voltage pattern at the nodes is the same and has a value decreasing with the length of the winding. To find out the rate of decline, the values of voltage at the nodes at the same time to be 1 μ s (the time when the voltage impulse reaches its maximum and is the most dangerous) are simulated by Matlab/Simulink software. These voltage values are shown in Table 3.

The voltage values at the 12 nodes are shown in Figure 16.

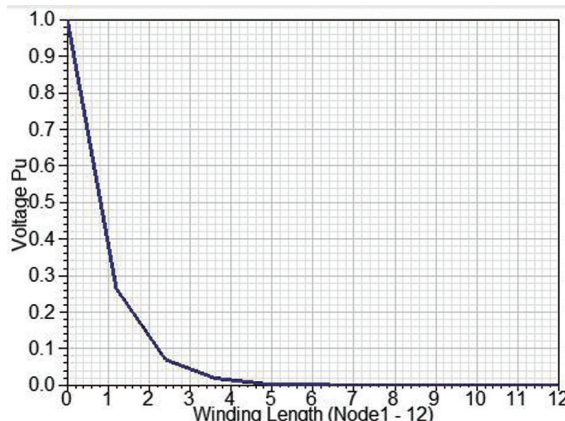


Figure 16. Voltage distribution at the 12 nodes at the time 1 μ s - continuous disk winding

Figure 16 shows that the initial voltage distribution of a continuous disk winding is in the form of a hyperbolic line which is different from the established voltage distribution line (straight line). The voltage has a very large value at the winding area between node 1 and node 2 (70%), this is the first gearing position. The rest of the winding is focused on 30% of the voltage. Uneven voltage distribution over a short period of time at the moment of transition causes insulation breakdown and failure in the transformer.

3.2.5. Obtained simulation results for interleaved disk winding type

Conducting the simulation for the case of interleaved disk winding type, the values of output voltage at the nodes depicted in Figure 17.

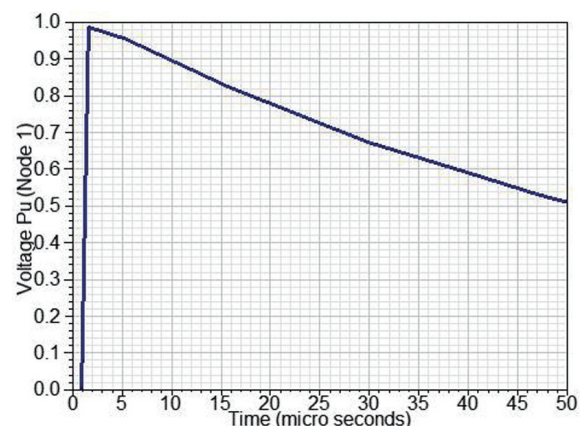


Figure 17. Voltage values at node 1 - Interleaved disk winding

Similarly, voltage values at the remaining 11 nodes are shown in Table 4.

Table 4. Voltage values at 12 nodes on interleaved disk winding

Node 1	Node 2	Node 3	Node 4	Node 5	Node 6
1.0000	0.7765	0.5968	0.534	0.4366	0.3023
Node 7	Node 8	Node 9	Node 10	Node 11	Node 12
0.213	0.1326	0.112	0.0856	0.0501	0.0324

The voltage values at the 12 nodes on the winding are shown in the graph in Figure 18.

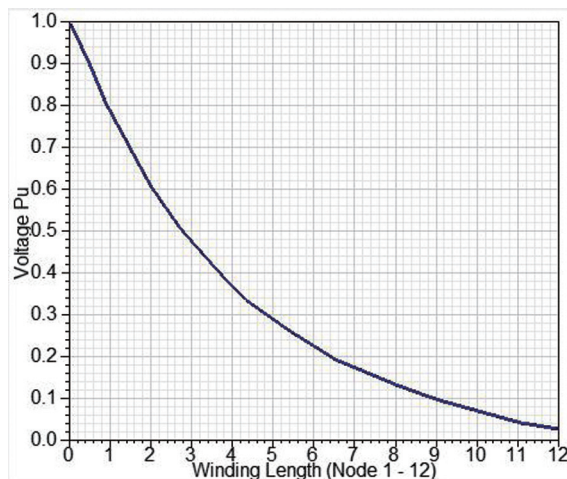


Figure 18. Voltage distribution at the 12 nodes at the time $1\mu\text{s}$ - interleaved disk winding

Figure 18 shows that the initial voltage distribution of the interleaved disk winding is close to the linearly stable distribution line. Compared with continuous disk winding, the voltage distribution on interleaved disk winding is better.

4. CONCLUSION

The paper used the state variable method solved on Matlab Simulink software to determine the voltage distribution across the nodes at any time and the voltage distribution across the winding at the time the lightning pulse voltage reaches its maximum value.

The paper has presented visual comparison results of the voltage distribution across two windings - continuous disk winding and interleaved disk winding. The results showed that the interleaved disk winding method has an initial voltage distribution close to that of a linearly stable distribution line. This means that the voltage distribution on the interleaved disk winding is more uniform than that on the continuous disk winding.

Compared with capacitance-related methods: using a capacitive ring, an electrostatic membrane, or adding capacitors to the winding, the interleaved disk winding method is much more effective in terms of improving the initial distribution voltage on the winding. Therefore, this method is commonly used for transmission transformers which are frequently affected by high voltage impulses or switching transients.

REFERENCES

1. Pham Van Binh and Le Van Doanh. Transformers - theory - operation - maintenance - test, Science and Technology publishing, Hanoi, 2011.
2. R. M. Del Vecchio, B. Poulin, R. Ahuja. Calculation and measurement of winding disk capacitances with wound-in-shields, *IEEE transactions on power delivery*, **1998**, 13(2), 503–509.
3. J. H. McWhirter, T. M. Ising, K. S. Kirk. Calculation of impulse voltage stresses in transformer windings, *IEEE proceedings transmission and distribution conference*, **1996**, 579–585.
4. S. V. Kulkarni, S. A. Khaparde. Surge Phenomena in Transformer, *Transformer engineering design and practice*, Indian Institute of Technology, Bombay, Mumbai, India, 2000, 277–326.
5. T. Wang, Z. Wang, Q. Zhang, L. Li. Measurement method of transient overvoltage distribution in transformerwindings, *2013 Annual report conference on electrical insulation and dielectric phenomena*, 1093–1096.
6. O. Moreau, P. Guuinic, R. Dorr, Q. Su, Comparison between the high frequency characteristics of transformerinterleaved and ordinary disk windings, *IEEE power engineering society winter meeting*, **2000**, 3, 2187–2192.
7. M. Heidarzadeh, M. R. Besmi. Influence of transformer layer winding parameters on the capacitive characteristic coefficient, *International journal on technical and physical problems of engineering*, **2013**, 5(15), 22-28.
8. M. Bagheri, A. Hekmati; R. Heidarzadeh; M. Salay Naderi, Impulse voltage distribution in intershield disk winding VS interleaved and continuous disk winding in power transformer, *IEEE 2nd International power and energy conference*, **2008**, 387-392.
9. M. Bagheri, M. S. Naderi, T. Blackburn, D. Zhang. Transformer Frequency Response Analysis: A mathematical approach to interpret mid-frequency oscillations, *2012 IEEE International conference on power and energy (PECon)*, 962–966.
10. M. Bagheri, B. T. Phung, T. Blackburn. Transformer frequency response analysis: mathematical and practical approach to interpret mid-frequency oscillations, *IEEE transactions on dielectrics and electrical insulation*, **2013**, 20(6), 1962–1970.